Available online at www.sciencedirect.com
SCIENCE DIRECT
Microporous and Mesoporous Materials 94 (2006) 234–242
MICROPOROUS AND MESOPOROUS MATERIALS
www.elsevier.com/locate/micromeso

# Cr(VI) immobilization in mixed (Mg, Al) oxides

S. Martinez-Gallegos [a,b], H. Pfeiffer [c], E. Lima [c,d,*], M. Espinosa [a], P. Bosch [c], S. Bulbulian [a]

[a] Instituto Nacional de Investigaciones Nucleares, Apdo. Postal 18-1027, C.P. 11801, México, DF, Mexico
[b] Facultad de Ciencias, Universidad Autónoma del Estado de México, Instituto Literario 100, C.P. 50000, Toluca, Edo. de México, Mexico
[c] Instituto de Investigaciones en Materiales, Universidad Nacional Autónoma de México, Ciudad Universitaria, C.P. 04510, México, DF, Mexico
[d] Departamento de Química, Universidad Autónoma Metropolitana-Iztapalapa, Av. San Rafael Atlixco 186, C.P. 09340, México, DF, Mexico

Received 2 February 2006; received in revised form 22 March 2006; accepted 29 March 2006
Available online 22 May 2006

**Abstract**

In the reaction sequence of thermal decomposition of chromate exchanged hydrotalcite a spinel structure was detected at 800 °C; the main compound was a periclase-like structure. At 1000–1200 °C the only compounds were MgO and the spinel $MgAl_{1.3}Cr_{0.7}O_4$. The particle size and morphology did not change with gamma irradiation or thermal treatments. The composition of the spinels $MgAl_{2-x}Cr_xO_4$ varies when samples are irradiated and/or thermally treated. Aluminum in octahedral sites is displaced to tetrahedral sites as chromium is incorporated into spinels. A molecular dynamics simulation of the spinels reproduced the experimental behaviour. A mechanism based on thermodynamical data and Wagner reactions is proposed.


*Keywords:* Chromium adsorption; Chromates; Hydrotalcite; Radiation damage; Spinel; Thermal decomposition

## 1. Introduction

Chromium is present in two oxidation states, trivalent and hexavalent. Cr(III) occurs naturally and it is an essential nutrient for humans. Instead, Cr(VI) is mainly produced as industrial effluents and it has to be retained [1–3] as it is carcinogenic to humans [1,4,5]. Those wastewaters are mainly due to leather and nuclear industry. If coming from nuclear wastes, the radioactivity is an added danger. There are not many strategies for Cr(VI) removal from wastewaters. One of them is the reduction of hexavalent chromium to trivalent with its subsequent immobilization as hydroxide.

Another procedure is its sorption onto various materials, including zeolites, hydrotalcite-like materials or activated carbon, among others [2,4,6,7]. These exchanged materials have to be treated to destroy their structure and to avoid the liberation of anions. Often, they are thermally treated. If the retained material is radioactive, the effect of radiation has also to be considered.

Layered double hydroxides or anionic clays, hydrotalcite-like materials, referred in this paper as hydrotalcites or HT, are of potential value in areas as diverse as catalysis, medicine, oil-field exploration or sorption processes [8]. Structurally, they consist of stacks of brucite-like $M(OH)_2$ layers in which a partial replacement of $M^{2+}$ by $M^{3+}$ occurs. The resulting charge on the layers needs the incorporation of charge-balancing anions ($A^{n-}$) such as carbonate, sulfate and hydroxide within the interlayer. In the general formula of HT, $[M^{2+}_{1-x}M^{3+}_x(OH)_2]A^{n-}_{x/n} \cdot mH_2O$ [9,10]; the two most common cations are magnesium-II and aluminum-III [11,12].

The thermal decomposition of HT can be described as a two-step mechanism. When the HT is heated in air up to 500 °C, it is transformed into a periclase-like Mg–Al oxide. In this case, the HT can be reconstructed by simple hydration. At temperatures higher than 500 °C, HT begins to produce magnesium oxide, MgO and the spinel $MgAl_2O_4$.

* Corresponding author. Address: Departamento de Química, Universidad Autónoma Metropolitana-Iztapalapa, Av. San Rafael Atlixco 186, C.P. 09340, México, DF, Mexico. Tel.: +525 58044667; fax: +525 58044666.
*E-mail address:* lima@xanum.uam.mx (E. Lima).

1387-1811/$ - see front matter © 2006 Elsevier Inc. All rights reserved.
doi:10.1016/j.micromeso.2006.03.045

If HT is thermally treated at temperatures higher than 800 °C, the HT cannot be reconstructed anymore [13] as the main compound turns out to be a spinel. The general formula of spinels, $AB_2O_4$, embraces a wide variety of A and B atoms. The valences of A and B can be 2 and 3 as in $MgAl_2O_4$ [14] which is constituted by a cubic close packed array of oxide ions with $Mg^{2+}$ in tetrahedral sites and $Al^{3+}$ in octahedral sites, each oxygen is surrounded tetrahedrally by three $Al^{3+}$ ions and one $Mg^{2+}$; as such, it is known as a normal spinel whose general formula is written as follows $A^{tet}B_2^{oct}O_4$. If the A ions and half B ions swap positions, the inverse spinel $B^{tet}[AB]^{oct}O_4$ is obtained. Intermediate spinels can have any cation arrangement between the extremes of normal and inverse spinels. Spinel, $MgAl_2O_4$, forms an extensive range of solid solutions with $Al_2O_3$ at high temperatures. If these $Mg^{2+}$ ions on tetrahedral sites are replaced by $Al^{3+}$ ions in the ratio 3:2 and the solid solution formula may be written $Mg_{1-3x}Al_{2+2x}O_4$, $x$ vacant cation sites, presumably tetrahedral ones, must therefore be present.

In a previous work, Martínez-Gallegos and Bulbulian [2] presented the ability of HT to retain Cr(VI) wastes. The HT with adsorbed chromate, also referred to in this paper as HT–Cr, was heated to immobilize Cr in the solid. The immobilization of chromium in the corresponding thermally treated solids was quantified in lixiviated liquors with a NaCl solution. It was found that γ-irradiation of HT–Cr samples developed a solid where chromium was retained more strongly than in the non-irradiated material. If heated at high temperature, samples, whether irradiated or not, immobilized the chromium (VI) originally present in the hydrotalcite in the form of Mg–Cr spinel. Although the thermal decomposition of different hydrotalcite-like materials has been reported [13,15–17], a detailed reaction sequence describing the thermal decomposition of HT–Cr has not been presented and radiation damage has not been discussed. The aim of the present study is first to obtain $CrO_4^{2-}$ adsorbed HT, then to investigate further the Cr immobilization in the thermally treated hydrotalcite and, lastly, to understand the structural effects of γ-irradiation.

## 2. Methods and materials

HT was produced as described previously by Sato et al. [18]. It was prepared by co-precipitating mixed metal solutions of magnesium and aluminum chlorides. One liter of an aqueous solution of 0.25 mol $AlCl_3$ and 0.75 mol $MgCl_2 \cdot 6H_2O$ was added dropwise to 1 L of an aqueous solution of 0.5 mol/L $Na_2CO_3$ and 2.5 mol/L NaOH under vigorous stirring for 3 h at 60 °C. The resulting precipitate was filtered and washed with deionized water to remove the chloride. Finally the powder was dried at 80 °C for 24 h.

The initial HT was thermally treated in a furnace at 500 °C for 3 h. Then, HT was reconstructed using 1 N ammonium chromate solution. The mixture was shaken for 24 h at room temperature and the solid was separated by centrifugation. It was then washed three times with deionized water. Fractions of this sample were heated at different temperatures, 500, 800, 1000 and 1200 °C in air for 3 h. A set of thermally treated HT–Cr samples was gamma-irradiated with a $^{60}Co$ gamma source in an industrial gamma radiator.

Chromium content in HT–Cr samples was determined by neutron activation analysis. The samples were irradiated in a TRIGA MARK III nuclear reactor for 30 min with an approximate neutron flux of $10^{13}$ n/cm$^2$ s. The 320 keV photo-peak, from the $^{51}Cr$ isotope produced by the nuclear reaction $^{50}Cr(n,\gamma)^{51}Cr$, was measured with a Ge/hyperpure solid-state detector.

The thermogravimetric (TG) analysis was performed in a TGA-51 TA Instruments Thermogravimetric Analyzer. The heating rate was 5 °C/min from room temperature to 1000 °C. Crystalline compounds were identified by X-ray diffraction (XRD), using a diffractometer (Siemens, D-5000) coupled to a copper anode X-ray tube. The $K_\alpha$ wavelength was selected with a diffracted beam monochromator. MgO which was found in all the XRD patterns, does not form solid solutions with Cr or Al at temperatures higher than 800 °C [19,20], hence, it was used in samples treated at 1000–1200 °C as an internal standard. The cell parameter $a$ of the spinel structure was determined from the (3 1 1) peak. Infrared spectra (FTIR) were obtained at room temperature with a Nicolet Magna-IR spectrometer, equipped with DTGS-CsI detector. The samples were diluted in KBr pellets. The resolution was 2 cm$^{-1}$. The different powders were studied by transmission electron microscopy (TEM) using a 1200-EX, JEOL instrument at 120 kV. The samples were prepared as specified in the standard powder methods.

$^{27}Al$ MAS NMR data were collected on a Bruker ASX300 spectrometer operating at 78.2 MHz. Samples were packed as powders into zirconia ceramic rotors. All samples were spun at 10 kHz. π/2 pulse was 2 μs with a recycling time of 0.5 s. $^{27}Al$ NMR signals were referenced relative to external 1 N aqueous $AlCl_3$.

All simulations were performed using the Cerius$^2$ software package [21], and the $MgAl_2O_4$ initial model was based on a reported structure [22]. The aluminum atoms were substituted by Cr atoms (0, 2, 4, 8, 12 and 16 atoms), into the theoretical cell, to generate different models. The theoretical study was performed using the energy minimization and dynamic simulation modules of Cerius$^2$ software.

## 3. Results

### 3.1. Elemental analysis

The HT thermally treated sample (500 °C/3 h) was left in the chromate solution for 24 h, in order to reach the maximum chromate absorption into the HT [23]. The amount of retained $CrO_4^{2-}$, measured by neutron activation analysis, was 3.2 meq per gram of calcined HT.

### 3.2. Composition

The XRD patterns of the HT and HT–Cr samples are compared in Fig. 1. Both samples may be identified as a hydrotalcite structure. However, while HT presents sharp and narrow peaks, the HT–Cr displays wide and not well defined peaks. Stanimirova et al. [24] have shown that the reconstructed HT corresponds to the rhombohedral polytype whose diffraction patterns exhibit broader peaks, independently of the initial sample. Furthermore, the peak (0 0 3) of the HT–Cr are clearly shifted to the left, indicating an increase in the interlamellar distance as the ionic radius of $CrO_4^{2-}$ (0.24 nm), is larger than that of $CO_3^{2-}$ (0.185 nm).

The HT–Cr samples were thermally treated at 500, 800, 1000 and 1200 °C. The XRD patterns of these samples are compared in Fig. 2. In the HT–Cr sample treated at 500 °C, MgO (JCPDS file 30-0794) [25] is the only identified crystalline phase. Actually, the composition of the MgO must correspond to the periclase material, $Mg_6Al_{2-x}Cr_xO_9$. When the sample is heated at 800 °C, periclase-like material is again the main phase, but small quantities of $MgAl_{2-x}Cr_xO_4$ spinel as a secondary phase are found as well. At 1000–1200 °C, the sample was crystalline and only MgO and $MgAl_{2-x}Cr_xO_4$ are found. The diffraction peaks, corresponding to the spinel containing Cr, are shifted about 0.5° in $2\theta$ to the left if compared to the $MgAl_2O_4$ spinel. Samples heated at 1200 °C present a better crystallization of the different phases, due to a sintering process.

The cell parameter $a$ for the $MgAl_2O_4$, is 0.809 nm (Fig. 3). It is in agreement with the $a$ value, 0.808 nm, reported in the JCPDS file 05-0672 [26]. Table 1 compares the cell parameter $a$ values of different $MgAl_{2-x}Cr_xO_4$ spinels to the value determined in our sample (0.816 nm). The ionic radius of Al is 0.675 nm which is lower than 0.755 (chromium radius). An expansion of the unit cell is, thus, expected. If a linear law is assumed (Végard law) between $x$ and the cell parameter $a$, the value of $x = 0.7$ is obtained for our spinel sample whose formula turns out to be $MgAl_{1.3}Cr_{0.7}O_4$. Therefore, the Cr/Al ratio is 0.54 which compared to the theoretical Cr/Al ratio in the fully exchanged HT (0.5) is 0.04 higher. Hence, some chromium should be adsorbed in some non-interlamellar exchange-

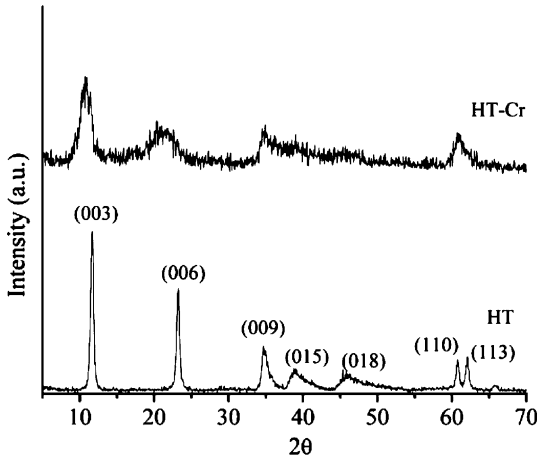


Fig. 1. X-ray diffraction patterns of the hydrotalcite as prepared (HT) and intercalated with chromium (HT–Cr).

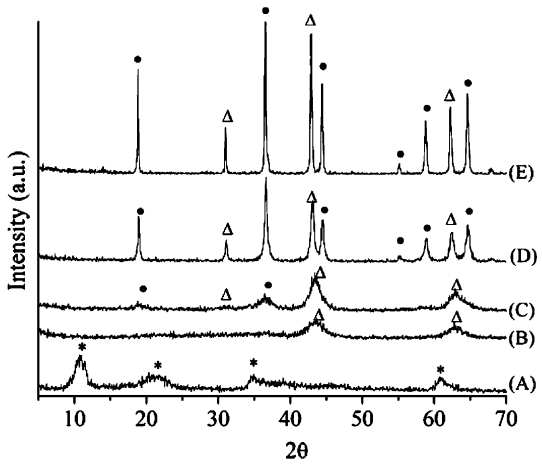


Fig. 2. X-ray diffraction patterns of the HT–Cr samples heated for 3 h at different temperatures. (A) Sample before the thermal treatment, (B) 500 °C, (C) 800 °C, (D) 1000 °C and (E) 1200 °C. Peaks were indexed as hydrotalcite (∗), MgO (△), $MgAl_{2-x}Cr_xO_4$ (●). Samples (C) and (E) were reported previously by Martinez-Gallegos and Bulbulian [2].

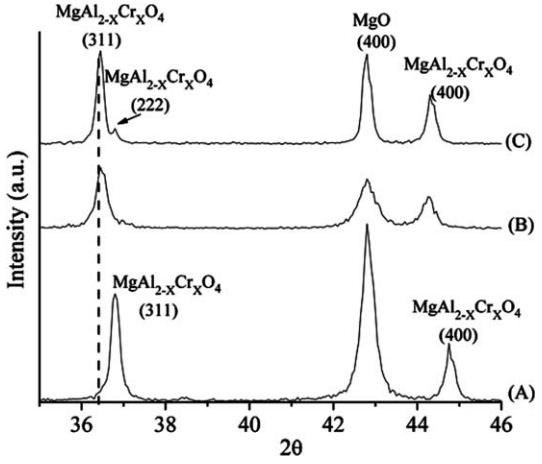


Fig. 3. X-ray diffraction patterns of the HT and HT–Cr samples treated at 1000 °C and 1200 °C, respectively. (A) HT at 1000 °C, (B) HT–Cr at 1000 °C and (C) HT–Cr at 1200 °C. Peaks were labelled with Miller index of indicated crystalline phase.

Table 1
$a$ cell parameter of $MgAl_{2-x}Cr_xO_4$ depending in $x$ value

| $MgAl_{2-x}Cr_xO_4$ | $a$ (nm) (JCPDS file) | $a$ (nm) ± 0.001 (this work) |
|---|---|---|
| $x = 0$ | 0.808 (file 05-0672) | 0.809[a] |
| $x = 0.5$ | 0.815 (file 23-1222) | – |
| $x = 1$ | 0.821 (file 23-1221) | – |
| $x = 0.7$ | – | 0.816[b] |
| $x = 2$ | 0.833 (file 10-0351) | – |

[a] Data measured from the HT treated at 1200 °C without Cr.
[b] Data measured from the HT treated at 1200 °C with Cr.

able sites of the HT, probably through a grafting process [27].

### 3.3. Theoretical model of the spinel structure

A theoretical model was developed in order to confirm the experimental composition obtained for the spinel structure. In the initial configuration of $MgAl_2O_4$, different amounts of Al atoms were substituted by Cr atoms, 0, 2, 4, 8, 12 and 16 atoms, where 0 and 16 correspond to $MgAl_2O_4$ and $MgCr_2O_4$, respectively. The minimum configuration energy was calculated for all the compositions. The results show that the cell parameter *a* increases as a function of the number of Cr atoms, as expected. The cell parameter changes from 0.806 nm to 0.839 nm as predicted by Végard rule (Fig. 4). The parameter *a* calculated for $MgAl_{1.25}Cr_{0.75}O_4$ was 0.818 nm. It is the closest simulated structure to $MgAl_{1.3}Cr_{0.7}O_4$ composition obtained experimentally. If the Al/Cr molar ratio in the simulation is higher than 1.25/0.75, i.e. one chromium atom added, the composition is $MgAlCrO_4$ which has been already reported (JCPDS card 23-1221). The parameter *a* for these two structures, experimental and theoretical, are in good agreement. Fig. 5 shows the theoretical XRD patterns for the $MgAl_2O_4$, $MgAl_{1.25}Cr_{0.75}O_4$ and $MgCr_2O_4$. When Cr is added into the spinel structure these XRD patterns present the same shift to the left. The intensity of the (222) peak is also a function of Cr amount. Therefore, Cr atoms are incorporated into the spinel structure and the cell parameter is altered due to the radius difference.

### 3.4. FTIR spectroscopy

Fig. 6 compares the IR transmission spectra for samples HT–Cr, non-thermally treated and thermally treated at 800 and 1200 °C. Spectra for these same samples irradiated at 6000 kGy are also included. The band due to $CrO_4^{2-}$ groups, Table 2, is clearly resolved at 887 $cm^{-1}$ for HT–Cr samples. This band vanishes when the sample is treated at 800 °C and a new weak band appears at 770 $cm^{-1}$. For samples treated at 1200 °C, the $CrO_4^{2-}$ band is no more present and the typical band attributed to $AlO_6$ groups in a spinel structure appears at 669 $cm^{-1}$ [28,29].

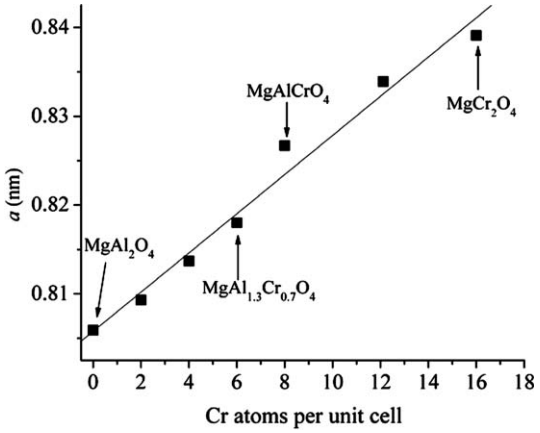


Fig. 4. Theoretical *a* cell parameters as a function of incorporated chromium.

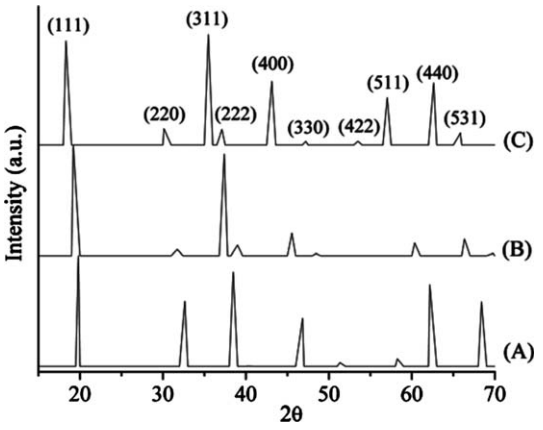


Fig. 5. Theoretical X-ray diffraction patterns of $MgAl_2O_4$ (A), $MgAl_{1.25}Cr_{0.75}O_4$ (B) and $MgCr_2O_4$ (C). Miller indexes correspond to spinel-like structure.

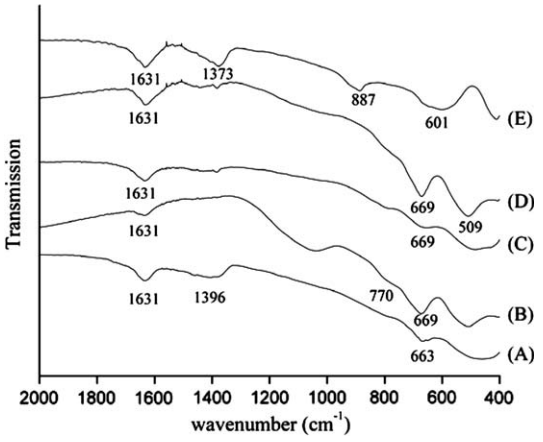


Fig. 6. FTIR spectra (A) HT–Cr – 800 °C, (B) HT–Cr – 1200 °C, (C) HT–Cr – 800 °C γ-irradiated at 6000 kGys, (D) HT–Cr – 1200 °C γ-irradiated at 6000 kGys and (E) HT–Cr, reported by Martinez-Gallegos and Bulbulian [2].

Table 2
Assignment of FTIR bands

| Species | Bond | Band ($cm^{-1}$) |
|---|---|---|
| $OH^-$ | O–H | 1631 |
| $CO_3^{2-}$ | C–O | 1373 |
| | C–O | 601 |
| $CrO_4^{2-}$ | Cr–O | 887 |
| $Cr_2O_3$ | Cr–O | 770 |
| $MgAl_{2-x}Cr_xO_4$ | Al–O | 669 |

### 3.5. Thermal behavior

Fig. 7 shows the TGA curves for HT and HT–Cr samples. Both hydrotalcites present similar trends, the first

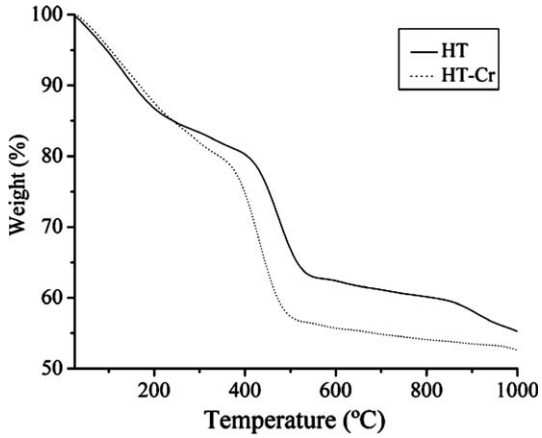


Fig. 7. TGA analyses of the HT and HT–Cr samples.

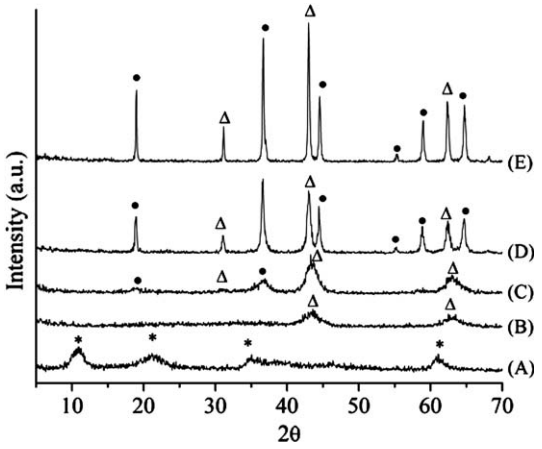


Fig. 8. X-ray diffraction patterns of the HT–Cr samples after the irradiation at 6000 kGy. The samples were previously treated for 3 h at different temperatures. (A) Sample before the thermal treatment, (B) 500 °C, (C) 800 °C, (D) 1000 °C and (E) 1200 °C. Peaks were indexed as hydrotalcite (∗), MgO (△), $MgAl_{1.3}Cr_{0.7}O_4$ (●). Samples (C) and (E) were previously reported by Martinez-Gallegos and Bulbulian [2].

weight loss of about 15 wt%, in both samples occurred between room temperature and 200 °C. This process is associated to the dehydration of the samples. A second weight loss is observed from 350 to 500 °C and it corresponds to a dehydroxylation process, attributed to periclase formation as discussed above (XRD). However, HT–Cr sample was dehydroxylated at higher temperature (410–540 °C) than HT sample (380–490 °C). Furthermore, the HT–Cr sample has ca. 8% less weight loss than sample free of chromium, in the region dehydroxylation. These effects could be due to the stabilization of the HT structure by $CrO_4^{2-}$ ions. Lastly, HT–Cr sample presented a third weight loss of about 5 wt% between 890 °C and 950 °C which is not present in the HT curve. This loss may be associated to the formation of the spinel structure, therefore to reduction of Cr(VI) to Cr(III).

### 3.6. Irradiated samples

#### 3.6.1. Composition

All the HT–Cr samples heated at different temperatures were irradiated with a $^{60}Co$ gamma source at 1000 kGy and 6000 kGy. Fig. 8 shows the XRD patterns of the samples irradiated at 6000 kGy. Although no new crystalline phases were detected as an effect of irradiation, if XRD patterns in Figs. 2 and 8 are compared, some differences are observed. Particularly, in the XRD patterns of samples heated at 1200 °C there is a change in the relative intensities between the peaks for $MgAl_{1.3}Cr_{0.7}O_4$ and the peaks for MgO. It seems that peaks for MgO increase their intensity as the sample is gamma irradiated. This is easily confirmed by comparing the intensities of peaks close to 36 (spinel) and 42 (magnesium oxide) at two theta. This result is discussed below. Furthermore, TEM studies show the same morphology before and after the irradiation process. No consolidation processes [30], due to irradiation are observed by TEM in these samples (Fig. 9). Both samples (HT–Cr treated at 800 °C before and after irradiation) present the same polyhedral morphology and particle size, 10–20 nm. However, when the samples are heated at 1200 °C, the particle size increases up to 1–2 μm due to the sintering process, as already mentioned in the XRD results.

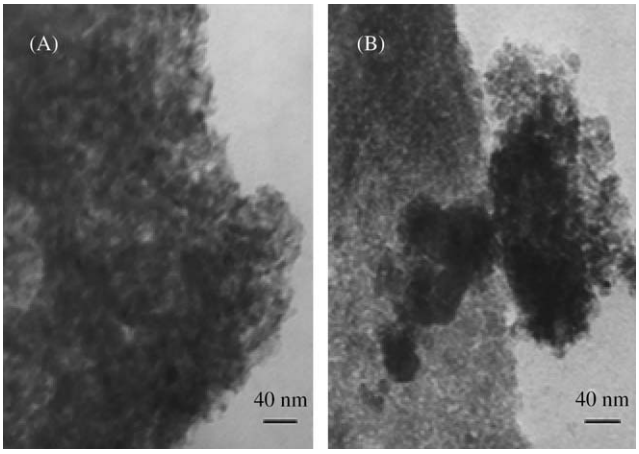


Fig. 9. TEM bright field images of the samples treated at 800 °C before (A) and after (B) the irradiation process at 6000 kGy.

From the FTIR spectra in Fig. 6, it could be inferred that gamma irradiation propitiates the spinel formation. In this sense, the area of the peak at 670 $cm^{-1}$ was compared with the area of the peak at 1361. The ratios of the peak areas are very close in the spectra A and B; C and D. Then, the FTIR data do not provide results showing, indisputably, the formation of spinel as a consequence of the gamma irradiation.

### 3.7. Aluminum coordination

The $^{27}Al$ MAS NMR spectra of samples HT and HT–Cr heated at 1200 °C, non-irradiated and gamma irradiated, are displayed in Fig. 10. These spectra exhibit signals close to 79, 68, and 7 ppm assigned to the presence of tetrahe-

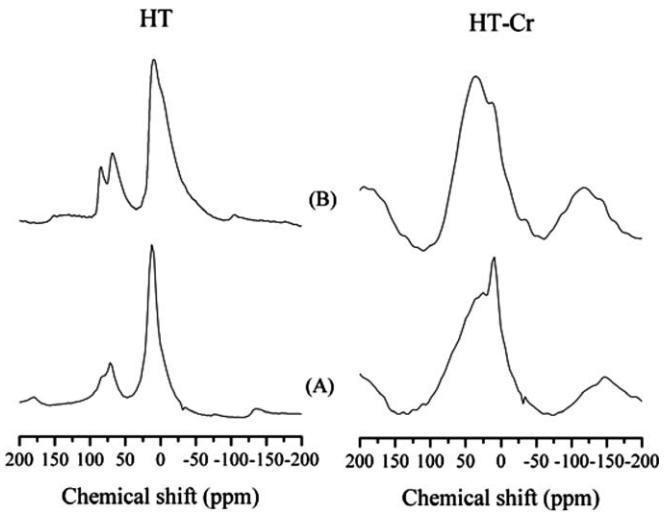


Fig. 10. $^{27}$Al MAS NMR spectra of HT and HT–Cr samples, treated at 1200 °C. (A) non-irradiated and (B) gamma irradiated at 6000 kGy.

dral, distorted tetrahedral and octahedral aluminum sites respectively in an oxygen environment [31,32]. The irradiation, as well as the incorporation of chromium, has an important effect on the distribution of aluminum species. Furthermore, irradiation and chromium incorporation promote the conversion of octahedral aluminum into tetrahedral aluminum, i.e., the aluminum is replaced by chromium; Fig. 10 shows that, as a consequence of irradiation, the signal attributed to octahedral aluminum is broadened. Thus, a coupling or paramagnetic effects due to presence of unpaired electrons in Cr(III), a $d^3$ configuration, is present.

## 4. Discussion

Results are summarized in Fig. 11. From the XRD and FTIR results, Cr is located between the layers of the reconstructed rhombohedral polytype HT. Still, small fractions of Cr must be retained in some external sites, according to Châtelet et al. [23]. The Mg/Al molar ratio is found to be 3 in both the original and the reconstructed HT, this is in good agreement with Stanimirova et al. [24] observations. Nevertheless, the Mg/Al molar ratio should increase with thermal treatment-reconstruction according to Mackenzie et al. [33].

The TGA analysis shows that the HT–Cr sample is more stable to thermal treatment than the HT sample. The dehydroxylation of the HT–Cr occurred at higher temperatures

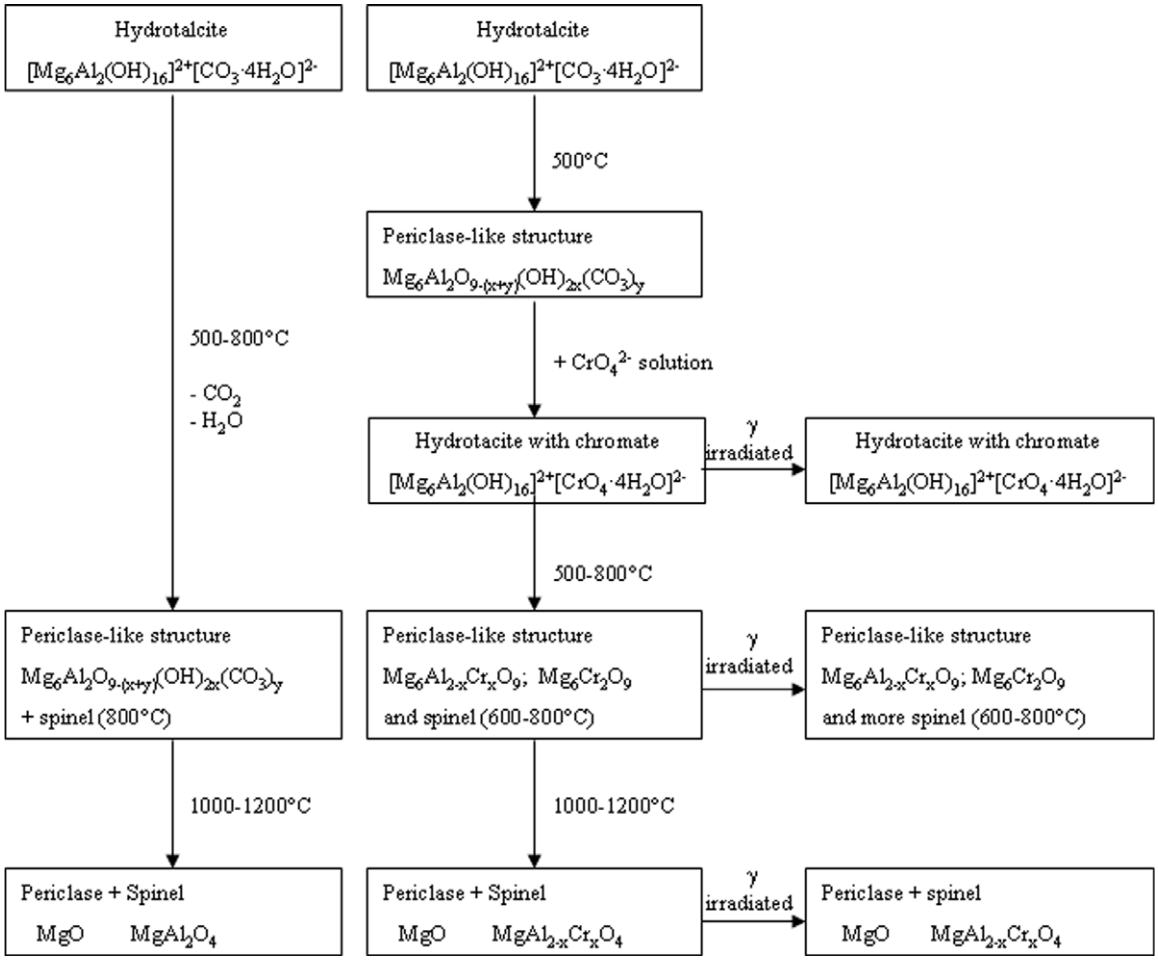


Fig. 11. Summarize of the thermal decomposition and radiation damage of HT–Cr samples.

than that of HT. These differences from 25 to 300 °C may be attributed to the difference in the structure, as reconstructed HT corresponds to the rhombohedral polytype [24]. Therefore, the bonds in HT–Cr are stronger and the ion diffusion is slow. At 500 °C, a periclase-like $Mg_6Al_{2-x}Cr_xO_9$ structure is formed which contains Al and Cr ions as mentioned by Stanimirova et al. [34]. Then, at higher temperatures, the spinel structure appears as the periclase-like structure content diminishes. These results are in agreement with the work of López-Salinas et al. [35]. FTIR spectroscopy confirms the XRD results as chromate infrared bands disappear and a new band at 770 $cm^{-1}$, attributed to the formation of the mixed oxide $Mg_6Cr_2O_9$, appears.

It seems that aluminum spinel is initially formed and chromium progressively becomes part of the structure if the following thermodynamical data [36] are considered:

$MgCr_2O_4$

$\Delta H^0_{298} = -1777.8$ kJ/mol

$C^0_p = 65.15 + 26.2 \times 10^{-3}\ T - 0.62 \times 10^6\ T^{-2}$ J/mol K

$MgAl_2O_4$

$\Delta H^0_{298} = -2299.1$ kJ/mol

$C^0_p = 146.78 + 35.56 \times 10^{-3}\ T - 3.68 \times 10^6\ T^{-2}$ J/mol K

The difference in $\Delta H^0_{298}$ of ≈500 kJ/mol favours the formation of the $MgAl_2O_4$. Therefore, the Cr stays on the periclase structure which surrounds the previously formed $MgAl_2O_4$ particles. Then, increasing the temperature these two oxides react forming the $MgAl_{2-x}Cr_xO_4$ and MgO. West [14] proposed the Wagner reactions to describe this process in MgO and $Al_2O_3$. If chromium is incorporated to this system, the following modified Wagner reactions may be proposed ($x = 1$, in $MgAl_{2-x}Cr_xO_9$):

(I) $Al^{3+} - Cr^{3+} + Mg_6Cr_2O_9 \rightarrow MgAlCrO_4 + 5MgO$

(II) $Cr^{3+} - Al^{3+} + MgAl_2O_4 \rightarrow MgAlCrO_4$

$Mg_6Cr_2O_9 + MgAl_2O_4 \rightarrow 2MgAlCrO_4 + 5MgO$

Reactions I and II correspond to the interfaces $Mg_6Cr_2O_9/MgAlCrO_4$ and $MgAlCrO_4/MgAl_2O_4$, respectively, Fig. 12. Therefore, from reaction I, while Al diffuses towards $Mg_6Cr_2O_9$, Cr diffuses in the opposite direction, and only in the interface described by reaction I, MgO is formed. Note that if MgO forms a continuous layer in the interface the chromium and aluminum diffusion would be impeded. Thus, as the periclase-like structure disappears the MgO must be forming isolated crystals.

Furthermore, this mechanism agrees with the calorific capacities, $C_p$, values. For a given amount of heat-energy, the temperature increase in the $MgAl_2O_4$ is higher, creating a thermal gradient in the interface, which favours chromium diffusion.

The spinel nuclei ($MgAl_{2-x}Cr_xO_4$) may be formed at or on the surface of the MgO crystals such that the oxide arrangement is essentially continuous across the MgO spinel interface. MgO constitutes the core of the particles, surrounded by the $MgAl_{2-x}Cr_xO_4$ spinel. Instead, Reaction II does not generate any MgO. In this reaction, Al diffuses from $MgAl_2O_4$ towards $MgAlCrO_4$, and Cr diffuses in the opposite way. This mechanism can be correlated to Fig. 13 reported by Martínez-Gallegos and Bulbulian [2]. They said that even at 800 °C Cr is partially lixiviated. In the proposed structure Cr remains at the surface as $Mg_6Al_{2-x}Cr_xO_9$, which following Stanimirova et al. [34], may rehydrate as HT.

In order to verify this hypothesis, an additional XRD pattern is presented in Fig. 14. It corresponds to the HT–Cr sample heated at 800 °C before and after lixiviation with 1 N NaCl solution. A small amount of hydrotalcite is recrystallized. The only anions available to reconstruct the layered structure are chlorides or chromates. The (0 0 3) distance obtained corresponds to chromate-exchanged hydrotalcite. Thus, a small amount of Cr(VI) is not reduced and it is located in the interlayer space of this hydrotalcite, therefore, chromium leaches from the solid in the form of $CrO_4^{2-}$ ions. This hydrotalcite may also recrystallize, partially, with chloride anions. This mechanism explains the results of Fig. 13.

In the irradiated samples, the spinel is homogenized as more Al is found in tetrahedral sites as determined by NMR. The aluminum species, or a fraction of them, that remain octahedrally coordinated are modified. Note, in Fig. 10, that in the corresponding spectra of HT samples, the signal close to 9 ppm is broader for the irradiated sample. Aluminum has a spin of 5/2 and possesses an electric quadrupole moment that can interact with the electric field gradients (EFG) at the nucleus. These quadrupolar effects are determined by the symmetry of the local surroundings of the nucleus. The EFG is more important at the surface

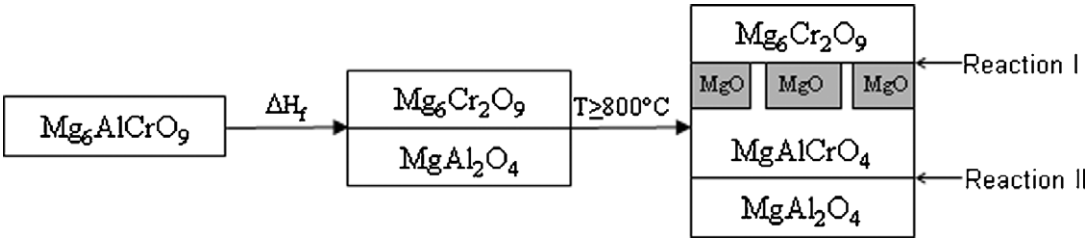


Fig. 12. Scheme of the modified Wagner reactions if $x = 1$ in the general formula $Mg_6Al_{2-x}Cr_xO_9$.

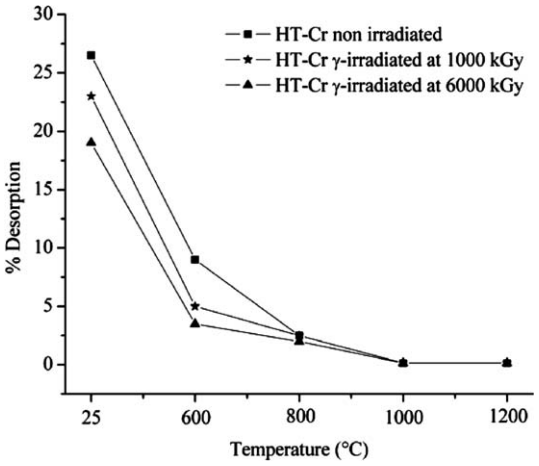


Fig. 13. Chromium desorption by lixiviation with a 1 N NaCl solution, taken from Martinez-Gallegos and Bulbulian [2].

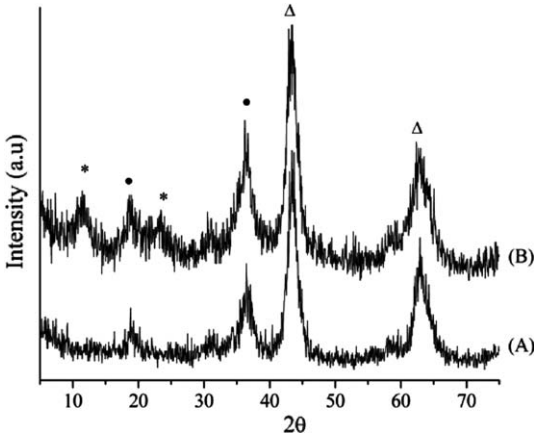


Fig. 14. X-ray diffraction patterns of the HT–Cr samples treated at 800 °C. (A) Before treatment with NaCl and (B) after treatment with NaCl. Peaks were indexed as hydrotalcite (∗), magnesium oxide (△) and spinel (●).

of the spinel and the broadening of the peak close to 9 ppm can be due to the segregation of aluminum in the Al containing compounds. A second hypothesis may be the creation of amorphous material. However, this last hypothesis is discarded because there is no evidence of amorphous material presence in XRD patterns.

Pells and Dupree et al. [37,38] have reported that irradiation produces ionization and displacement damage in spinel structure. These works propose the creation of octahedral cation vacancies as a consequence of the displacement of the aluminum by magnesium. The appearance of these vacancies can be responsible of the modification of the NMR signal corresponding to octahedral aluminum.

Then, the spinel structure initially tends towards a normal spinel, but gamma irradiation increases spinel inversion. A similar behavior has been observed in magnesium–aluminum spinel irradiated by neutrons.

## 5. Conclusions

HT–Cr decomposed when it was heated at 800 °C or higher temperatures in air. A periclase-like $Mg_6Al_{2-x}Cr_{2x}O_9$ structure is produced. HT–Cr decomposes through a complex mechanism, including the formation of the $MgAl_{1.3}Cr_{0.7}O_4$ spinel and MgO at 1000–1200 °C. Gamma irradiation of HT–Cr causes displacement of aluminum from octahedral to tetrahedral sites as shown by $^{27}Al$ NMR. These results may be interpreted through Wagner reactions which show that MgO is only synthetized at the $Mg_6Cr_2O_9/MgAlCrO_4$ interface. Furthermore, according to thermodynamical data $MgAl_2O_4$ is first produced. Later Cr diffuses through the $MgAl_2O_4$ in order to produce the $MgAl_{2-x}Cr_xO_4$ spinel.

When the $MgAl_{2-x}Cr_xO_4$ external layer in the HT–Cr thermally treated at 800 °C is in contact with a NaCl solution, HT recrystallizes and residual Cr(VI) occupies the interlayer space.

## Acknowledgements

This project was supported by CONACYT Mexico, project 32096-E. S. Martínez-Gallegos thanks CONACYT for financial support. The technical work of C. Flores in TEM is gratefully acknowledged.

## References

[1] N.K. Lazaridis, D.D. Asouhidou, Water Res. 37 (2003) 2875.
[2] S. Martinez-Gallegos, S. Bulbulian, Clays Clay Miner. 52 (2004) 651.
[3] S. Martinez-Gallegos, V. Martinez, S. Bulbulian, Separation Sci. Technol. 39 (2004) 667.
[4] R.L. Goswamee, P. Sengupta, K.G. Bhattacharyya, D.K. Dutta, Appl. Clay Sci. 13 (1998) 21.
[5] N.K. Lazaridis, T.T. Pandi, K.A. Matis, Ind. Eng. Chem. Res. 43 (2004) 2209.
[6] E. Cooney, B. Luo, J.W. Patterson, C. Petropoulou, in: D.L. Ford (Ed.), Water Quality Management Library, vol. 3, P.T. Lancaster, Sta. Fe., New Mexico, 1992, p. 109.
[7] E. Chiemlewska, Turk. J. Chem. 27 (2003) 639.
[8] S.P. Newman, W. Jones, P. O'connor, D.N. Stamires, J. Mater. Chem. 12 (2002) 153.
[9] F. Cavani, A. Trifiro, A. Vaccari, Catal. Today 11 (1991) 2.
[10] S. Miyata, Clays Clay Miner. 28 (1980) 50.
[11] H.C.B. Hansen, R.M. Taylor, Clay Miner. 26 (1991) 311.
[12] G. Fetter, E. Ramos, M.T. Olguín, P. Bosch, T. López, S. Bulbulian, J. Radioanal. Nucl. Chem. 221 (1997) 63.
[13] T. Hibino, A. Tsunashima, Clays Clay Miner. 45 (1997) 842.
[14] A.R. West, Solid State Chemistry and its Application, John Wiley Sons, New York, 1990.
[15] M.J. Kang, S.W. Rhee, H. Moon, Radiochim. Acta 75 (1996) 169.
[16] T. Hibino, K. Kosuge, A. Tsunashima, Clays Clay Miner. 44 (1996) 151.
[17] F.M. Labajos, V. Rives, Inorg. Chem. 35 (1996) 5313.
[18] T. Sato, H. Fujita, T. Endo, M. Shimada, A. Tsunashima, React. Solids 5 (1988) 219.
[19] W.T. Wilde, W.J. Rees, Trans. Brit. Ceram. Soc. 42 (1943) 127.
[20] C. Greskovich, V.S. Stubican, J. Amer. Ceram. Soc. 51 (1968) 42.
[21] Cerius 2. Molecular Simulations Inc., San Diego, 1999.
[22] H. Sawada, Mater. Res. Bull. 30 (1995) 341.

[23] L. Châtelet, J.Y. Bottero, J. Yvon, A. Bouchelaghen, Colloids Surf. A: Physicochem. Eng. Aspects 111 (1996) 167.
[24] T.S. Stanimirova, G. Kirov, E. Donolova, J. Mater. Sci. Lett. 20 (2001) 453.
[25] A. Freund, Ber. Dtsch. Keram. Ges. 47 (1970) 739.
[26] D. Swanson, S. Fuyat, Natl. Bur. Stand (US), Circ. 539 (2000) 11.
[27] F. Malherbe, J.P. Besse, J. Solid State Chem. 155 (2000) 332.
[28] D.S. Ross, Inorganic Infrared and Raman Spectroscopy, McGraw Hill, London, Great Britain, 1972, pp. 112–117.
[29] M.F.M. Zawrah, A.A. El Keshen, Brit. Ceram. Transitions 101 (2002) 71.
[30] L. Yang, R. Medico, W. Baugh, K. Schultz, J. Nucl. Mater. 103 (1981) 585.
[31] A. Samoson, E. Lippmaa, Phys. Rev. B 28 (1983) 6567.
[32] A. Samoson, E. Lippmaa, G. Engelhardt, U. Lohse, H. Jerschkewitz, J. Chem. Phys. Lett. 134 (1987) 589.
[33] K.J. Mackenzie, R.H. Meinhald, B.L. Sherriff, Z.J. Xu, J. Mater. Chem. 3 (1993) 1263.
[34] T.S. Stanimirova, I. Vergilov, G. Kirov, N. Petrova, J. Mater. Sci. 34 (1999) 4153.
[35] E. López-Salinas, E. Torres-García, M. García-Sánchez, J. Phys. Chem. Solids 58 (1997) 919.
[36] M. Binnewlers, E. Milke, Thermochemical Data of Elements and Compounds, J.W. Sons, New York, 2002, p. 207.
[37] G.P. Pells, J. Nucl. Mater. 184 (1991) 177.
[38] R. Dupree, M.H. Levis, S.M. E, Philos. Mag. A 53 (1986) L-17.